

Linking ecosystem dynamics and biogeochemistry: Sinking fractionation of organic carbon in a Swedish fjord

Anya M. Waite¹

Centre for Water Research, University of Western Australia, 35 Stirling Highway, Crawley, 6009 Western Australia, Australia

Örjan Gustafsson

Stockholm University, Institute of Applied Environmental Research (ITM), SE-10 691 Stockholm, Sweden

Odd Lindahl

Royal Swedish Academy of Sciences, Kristineberg Marine Research Station, SE-450 34 Fiskebäckskil, Sweden

Peter Tiselius

Department of Marine Ecology, Göteborg University, Kristineberg Marine Research Station, SE-450 34 Fiskebäckskil, Sweden

Abstract

We studied the growth and sedimentation of a phytoplankton bloom in the Gullmar Fjord in spring 2001. Sinking fractionation, as measured by differential sinking of components having varied carbon isotope signals, was an important process in determining carbon fluxes within this complex coastal ecosystem. Large, rapidly sinking diatoms aggregated with their own carbon exudates. This exudate material was the single largest contributor to vertical carbon flux in the fjord over the study period, and amounted to an order of magnitude greater carbon flux than the live biomass reaching the sediment traps. We estimate that diatoms' primary production contributed 75% of the total integrated production, ~100% of new production and ~100% of the total sedimentary flux during the primary sedimentation event, despite the fact that the surface bloom biomass was dominated by high concentrations of the flagellate *Chattonella* sp. Diatoms carried a heavy carbon isotope signature ($\delta^{13}\text{C} = -19\text{‰}$) to depth; this moved downward as a layer through the water column, distinct from other particular organic carbon (POC) at the surface having a very light signature (-23 to -26‰). This light $\delta^{13}\text{C}$ signature at the surface coincided with a surface peak in particulate and dissolved organic carbon (POC/DOC) and transparent exopolymer particles (TEP), and material carrying the low $\delta^{13}\text{C}$ signature had a negligible sinking rate. This distinctive surface signature probably contained small POC typical of the microbial loop and its products, a component of which was the very low -32‰ of the organic colloids. Measurable aggregation of these colloids occurred, and they may have contributed up to ~20% of the vertical flux very early in the study. Sinking fractionation of POC caused isotope composition shifts on the order of 3–7‰.

One of the key challenges in understanding the aquatic carbon cycle is the functional separation of suspended and sinking particles in surface waters (Gardner 1997; Gustafsson and Gschwend 1997). Predicting organic carbon fluxes from surface waters has been identified as a high priority in the study of global climate change (Berger et al. 1989; Sarmiento 1991), and is also important with regard to the global fate of vital elements associated with organic carbon (N, P, Si, Fe, Cu, and Co; e.g., Sarmiento 1991; Hedges 1992) as well as for ecosystem longevity of persistent organic pollutants (Axelman and Gustafsson 2002).

The growth of phytoplankton in surface waters represents

one of the largest single transfers of marine carbon on an annual time scale. The fate of this carbon directly impacts microbial communities (Smith 2002), pelagic and benthic grazers (Hasegawa et al. 2001; van de Bund et al. 2001), and benthic ecosystems as a whole (Hee et al. 2001). The ecological fate of this carbon hinges largely on its partitioning between suspended and sinking matter (Waite et al. 1992a). Individual sinking events are governed by particle dynamics that are both biological and physical-chemical in nature (e.g., Chin et al. 1998). For example, phytoplankton cell aggregation can trigger rapid sedimentation of phytoplankton carbon from the surface mixed layer; and the timing and extent of such flux events can distort nutrient budgets (Jackson and Lochmann 1992), determine which predators target the phytoplankton as a food source (van de Bund et al. 2001), and skew the fraction of production which becomes incorporated into sediments (Kemp and Baldauf 1993), an important factor to consider in climate hindcasting (Lange et al. 1990). It has recently been noted that dissolved and colloidal organic carbon can independently aggregate

¹ Corresponding author (waite@cwr.uwa.edu.au).

Acknowledgments

We thank B. Alexander, K. McMahon, E. Zelander, Z. Kukulska, and J. Larsson for assistance in the field.

The Swedish Research Council (NFR grant 1-AA/GB 12291–301) and the Australian Research Council (ARC Large A00001248) supported this work.

into particles that represent food sources for grazers without the (often assumed) intermediary step of bacterial processing, short-cutting the microbial loop (Kerner et al. 2003).

The study of particulate organic matter (POM) flux in aquatic systems now requires integrated and multidisciplinary approaches. Biogeochemical characterization of ecosystems (Dafner and Wangersky 2002; Volkman and Tanoue 2002) has been coupled with the suspension characteristics of key organisms (Moore and Villareal 1996). The use of stable isotope analysis is becoming more widely applied to increase understanding of some of the chemical patterns embedded within ecosystems (e.g., McClelland and Montoya 2002; Volkman and Tanoue 2002). Recent advances in high-resolution video (Davis et al. 1992; Waite et al. 1997b), sediment trap techniques (Waite et al. 2000), and particle fractionation (Gustafsson et al. 2000 on coupled cross-flow filtration-split flow thin-cell fractionation [CFF-SPLITT]) have provided tools for a broader understanding of the relationship between the flux of particles from ecosystems and the function of organisms within ecosystems. Such biogeochemical understanding is necessary to predict longer-term changes in the biogeochemical state of the world ocean (Doney 1999).

Here we use a combination of particle fractionation techniques, sinking rate measurements, and biological and geochemical measurements to explore linkages between the ecology and biogeochemistry of a coastal fjord during the spring period immediately after the spring bloom, when new material is available for export. We investigate in particular how the growth and sinking properties of phytoplankton and other organisms contribute to the vertical fractionation of the geochemical signals (primarily the stable carbon isotope signature) in the fjord.

Methods

Field sampling—Between 13 March and 4 April 2001, we sampled the water column three times per week at a station in the central Gullmar Fjord, Sweden, depth 50 m (Alsback: 58°19.0'N, 11°32.0'E). All field operations were based at the Kristineberg Marine Research Station (KMRS) near Fiskebäckskil. Sampling was undertaken from KMRS's research vessel Arne Tiselius, and included conductivity, temperature, depth sensor casts and Niskin bottle sampling at 8–10 depths from 0 to 50 m, with more detailed sampling in the mixed layer. Subsamples from each depth were filtered (on GF/F filters) for chlorophyll *a* (Chl *a*) and particulate organic carbon and nitrogen analyses (POC and PON), including $\delta^{13}\text{C}$ and $\delta^{15}\text{N}$ analyses. These were desiccated and frozen until analysis at the shore laboratory. Filtrate was retained for several rinses of 25-ml vessels before the sample was taken and frozen for nutrient analysis. Cell count samples were taken at the surface (0 m) and at the chlorophyll maximum (2–5 m) as indicated by the fluorescence trace. A sampling hose was also lowered to 15 m to yield integrated mixed layer samples for cell count analysis and for several biogeochemical measurements (below). All cell count samples were preserved in Lugols for later analysis. Ten-liter samples from the chlorophyll maximum depth were retained for later sinking rate measurements in the laboratory.

Chl *a* samples were ground and extracted in 10-ml acetone and analyzed immediately for Chl *a* concentration on a Turner Designs AU-10 fluorometer (Parsons et al. 1984). Particulate carbon samples were first mildly acidified in Ag capsules and then analyzed for POC, PON, $\delta^{13}\text{C}$, and $\delta^{15}\text{N}$ as follows: stable isotope abundances and ratios of carbon and nitrogen were measured by continuous flow isotope ratio mass spectrometry (20–20 mass spectrometer, PDZEuropa) after sample combustion to CO_2 and N_2 at 1,000°C in an on-line elemental analyzer (PDZEuropa ANCA-GSL). The gases were separated on a Carbosieve G column (Supelco) before introduction to the isotope ratio mass spectrometer (IRMS). Sample isotope ratios were compared to those of standard gases injected directly into the IRMS before and after the sample peaks, and $\delta^{15}\text{N}$ (vs. AIR) and $\delta^{13}\text{C}$ (vs. PDB) values were calculated.

Dissolved nutrients were analyzed on a Traacs 800 Autoanalyser. TEPs were measured after 19 March on Niskin bottle samples from all depths to 30 m using the Alcian Blue method of Passow and Alldredge (1994). Phytoplankton and ciliates were preserved with acetic Lugol solution, and cells larger than 10 μm were counted by the Utermöhl technique (Utermöhl 1958) using a Leitz DMRIB microscope on integrated hose samples and on samples from the fluorescence maximum. For each species, phytoplankton carbon was calculated by multiplying cell concentrations for that species by the estimated carbon content pg C cell^{-1} from Edler (1977). Where unavailable, the carbon content was estimated from that of the most closely related species.

For the analysis of dissolved organic carbon (DOC), 10 ml of the seawater was collected in duplicate 15-ml acid-washed HDPE test tubes (Falcon) and acidified with 100 μl of 1 mol L^{-1} HCl. The samples were analyzed with high-temperature catalytic oxidation technique on a Shimadzu TOC-5000 instrument.

Integrated net primary production was measured over a longer time period than other measurements, weekly beginning 12 February 2001 and continuing though to 18 April 2001, as part of a long-term sampling program of O. Lindahl. During the main part of the study (13 March through 4 April 2001), integrated net primary production was measured using ^{14}C on each sampling day, according to the protocol developed by Lindahl (1995). Samples from 5 depths were incubated in situ at 9 depths down to 15 m for 4 h around noon on a mooring adjacent to KMRS near the fjord sill (Pricken: 58°15.5'N, 11°27.2'E).

Zooplankton samples for abundance estimation were collected with vertical hauls (0–30 m) using a 200 μm WP-2 net equipped with a General Oceanics flow meter. Samples were preserved in 5% formaldehyde and after subsampling (1/10) analyzed for abundance, species composition, and prosome length. Dry weights were estimated from regressions in Klein Breteler and Gonzalez (1982) and Bottrell and Robins (1984) and converted to carbon assuming a carbon/dry weight ratio of 0.45.

Water samples for fecal pellet abundance were taken with a rosette at trap depths (15, 30, and 50 m). One liter of sampled water was sieved through a 20 μm sieve, and pellets were retrieved and counted within 4 h of collection. (Size distribution of pellets was estimated from measuring 20 pel-

lets from each sample.) Carbon content of pellets was estimated from pellet volumes and a conversion factor $0.057 \text{ mg C mm}^{-3}$ (Gonzalez and Smetacek 1994).

Sediment traps—Individual cylindrical 8 cm diameter by 55 cm high sediment traps were deployed at the study site at 15, 30, and 50 m on a single mooring. Traps were collected, emptied, and redeployed on each sampling date. Measurements included bulk POC, PON, and $\delta^{13}\text{C}$ and $\delta^{15}\text{N}$ analysis; species composition counts; and gel analysis of particle size and type (Waite et al. 2000).

Sinking rate measurements—On each sampling day, bulk sinking rate measurements were made on samples taken at the fluorescence maximum (F_{max}) as indicated by the in situ fluorometer trace (generally 2–5 m depth), using the SETCOL method (Bienfang 1981) as modified by Waite et al. (1992b). In separate experiments we used carbon (POC), chlorophyll *a*, and phytoplankton species cell counts (as above) as biomass indicators for sinking rates. Video sinking rate measurements of individual suspended particles were executed according to the method of Waite and coworkers (unpubl. data).

Sinking fractionation measurements—Settling columns were filled with filtered seawater to the top spigot of the settling column using a salinity gradient to ensure column stability (Waite et al. unpubl. data). Concentrated samples of the fraction of interest were then layered above the top spigot. The sample was left to settle for 12 h, and three samples were collected through the top, middle, and bottom spigots, respectively. The timing was such that all particles reaching the bottom fraction must have sunk at a rate greater than 1 m d^{-1} . This settling velocity was chosen based on geochemical inferences that suggest such slow transport is important for export of particles from surface water. From a ^{238}U – ^{234}Th disequilibrium of about 50%, which was found in Gullmar Fjord (Gustafsson et al. unpubl. data) and in other coastal regimes, a piston velocity for settling of 1 m d^{-1} may be calculated for the particle-associated ^{234}Th . It has also been independently verified using SPLITT techniques that the 1 – 2 m d^{-1} is an important range for the settling POC in shelf waters (Gustafsson et al. 2000). Particles still in the top fraction at the end of the experiment were considered neutrally buoyant, while particles in the middle fraction were settling at a rate of less than 1 m d^{-1} . Collected fractions were analyzed for POC and PON, and $\delta^{13}\text{C}$ and $\delta^{15}\text{N}$ as above. Sinking experiments were performed on several bulk samples collected at 5 m, on a greater than $90 \mu\text{m}$ net haul containing almost pure *Coscinodiscus concinnus* and *Coscinodiscus centralis* on 28 March, and on a sample collected as bulk retentate from 800 liters in a specially designed all stainless steel and ceramics high-capacity $0.22 \mu\text{m}$ cross-flow filtration unit (Ceraflo TFF, Millipore AB), which has been described in detail elsewhere (Broman et al. 1996). This latter fraction was tinted yellow in color, indicating the high concentration of organic matter fraction above $0.22 \mu\text{m}$. Though collected from waters containing significant numbers of *C. concinnus* and *C. centralis* (above), microscopic observation indicated that this fraction did not contain whole

cells, although frustule shards were visible. We assume that this particular design of high-volume pump did not successfully retain the integrity of these largest particles ($>90 \mu\text{m}$).

Flocculation experiments—Flocculation experiments were executed using video measurement of particle size, according to the method of Waite et al. (1997b), in a Couette cell of 1 liter water volume. In one case, we executed a DOC flocculation experiment to measure the extent to which sub-micron carbon compounds (colloidal carbon [COC]) could flocculate into filterable particles under shear (5 s^{-1}). Here, we prepared a series of 1-liter samples of raw 5-m seawater filtered through a $0.22\text{-}\mu\text{m}$ membrane filter. Filtered samples were then placed in the Couette cell for 0, 1, 2, 4, and 9 h, followed by filtration onto a GF/F filter ($\sim >0.7 \mu\text{m}$). The GF/F filter was then analyzed for POC and PON, $\delta^{13}\text{C}$ and $\delta^{15}\text{N}$ as above. In this manner we could also measure the isotopic signature of the flocculated COC.

Results

Water mass movement—The temperature and salinity characteristics of the Gullmar Fjord during the period of the study show that surface, middepth, and deep-water masses almost always carried distinct water signatures, indicating a different oceanographic origin (Fig. 1A). Deep waters (35–50 m) had the most constant properties, being relatively warm (4 – 6°C) and saline (33–35‰), characteristic of bottom water winter inflows from the Skagerrak/North Sea (Lindahl 1987). Middepth waters were less saline (25–33‰), characteristic of intermediate salinity water from the Jutland current, and showed a progressive warming and freshening with time. Surface waters were distinctly cooler and fresher than middepth or bottom waters, typical of Baltic outflows that mix with Kattegat and Skagerrak water. Most of the density stratification was driven by salinity.

Two distinct increases in middepth temperature during the study (19 March and 2 April 2001) divide the study period into three intervals of relatively constant water mass composition: 13–16 March, 19–30 March, and 2–4 April (Fig. 1B). We will focus most of our analysis on the longest period of relatively constant water mass composition, 19 March–30 March.

An upwelling event occurred before and during 19 March, bringing saline, nutrient-rich water closer to the surface (Fig. 2A) and displacing the fresher surface layer. This was preceded by several days of easterly winds, known to cause upwelling (Lindahl 1987). All changes in biomass must therefore be viewed against this physical backdrop (Chl *a*, particulate organic carbon and nitrogen [POC and PON]; Fig. 2B–D).

Surface nitrate concentrations had already been significantly depleted upon our arrival at the study site on 14 March, indicating biological nutrient drawdown in previous days/weeks consistent with an earlier increase in surface productivity (Waite and Lindahl unpubl. data). Relaxation of the upwelling brought significant decline in nutrient concentrations via dilution with nutrient-poor surface water, as well as probable drawdown from biological causes (Fig. 2A). To separate observed declines in nitrate due to biological draw-

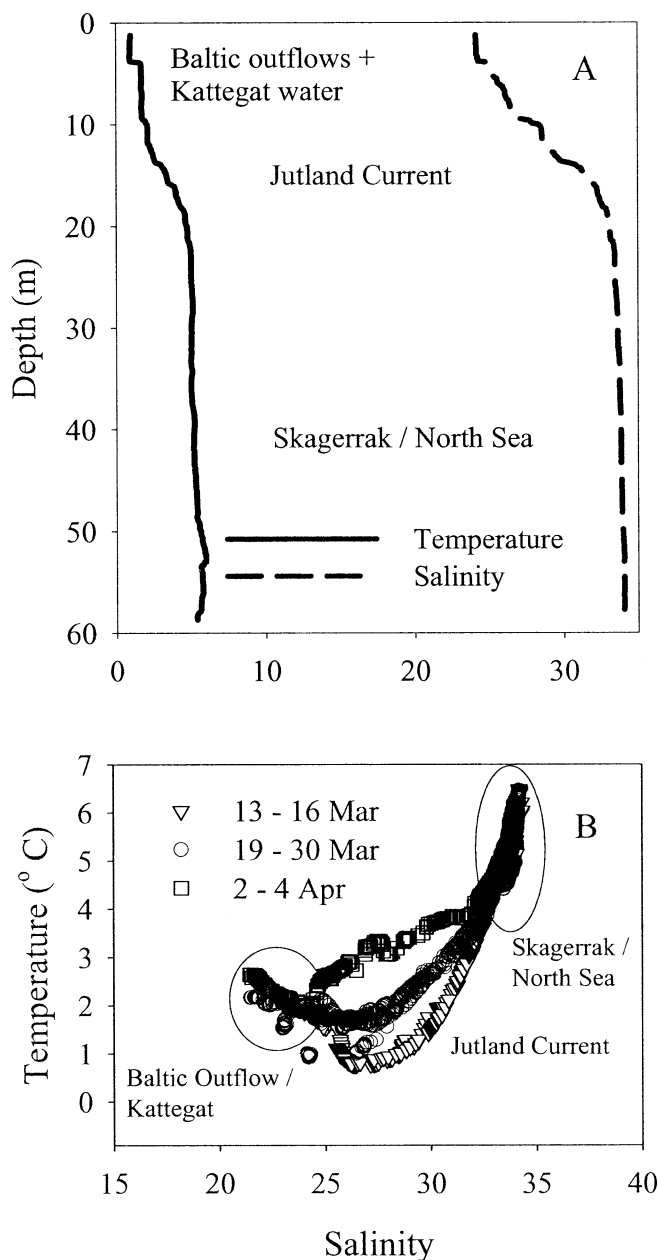


Fig. 1. (A) Typical temperature (T) and salinity (S) profile for the Gullmar Fjord in the middle of the sampling period (14 March through 4 April 2001). Surface waters contain water flowing seaward from the Baltic mixed with waters of the Kattegat. The Jutland Current, coming north from Denmark, forms the middle layer. Deep waters are typical in T and S characteristics of the more saline North Sea underflow and Skagerrak. (B) Temperature versus salinity plot showing the different T/S characteristics of the three water masses. Changes in middepth water mass occurred twice over the period of the study (19 Mar 2001 and 2 Apr 2001), but were relatively constant 19 Mar through to 30 Mar 2001, the main period over which our analysis is focused.

down from those related to the relaxation of the upwelling, we plotted $[\text{NO}_3 + \text{NO}_2]$ (referred to hereafter as $[\text{NO}_3]$) versus salinity for surface waters 0–10 m, including two deeper depths on 16 March, the sampling day just before

peak upwelling (Fig. 3). We use the straight-line relationship between nitrate and salinity on 16 March as an estimate of the basic dilution of NO_3 occurring as saline water rich in NO_3 mixes with fresher, more nutrient-poor surface water. Changes in $[\text{NO}_3]$ along this line should indicate changes in $[\text{NO}_3]$ due to dilution and/or upwelling, whereas reductions in $[\text{NO}_3]$ at a single salinity (Fig. 3) can be clearly attributable to other non-mixing-related causes such as biological uptake. On this basis we infer a conservative estimate of biological drawdown of $2 \mu\text{mol L}^{-1}$ nitrate from 19 March until it became nondetectable over the top 20 m on 30 March. This would indicate a total drawdown of $40 \text{ mmol m}^{-2} \text{NO}_3$, roughly 0.56 g N . If we assume assimilation of nutrients at the Redfield ratio (C:N = 6.625:1), this could possibly support up to $\sim 3.2 \text{ g C m}^{-2}$ as New Production integrated 0–20 m.

Chl *a* profiles indicated an early surface peak (Fig. 2B), dissipated by upwelling on 19 March, and followed by the redevelopment of a strong surface peak 21 March through to 4 April. A large subsurface peak at 30 m on 14–16 March suggested the presence of a relic sedimentation event from an earlier diatom bloom (see *Species Composition* below), and a smaller deepening of the chlorophyll contours to 20 m on 30 March was also possibly suggestive of a sedimentation event. Surface Chl *a* was reasonably constant ($8\text{--}20 \mu\text{g L}^{-1}$) and, except for the sedimentation events, generally declined exponentially with depth. Integrated productivity was low mid-February ($127 \text{ mg m}^{-2} \text{ d}^{-1}$ on 13 February), increasing in late February/early March, with peak production on 16 March ($1,059 \text{ mg m}^{-2} \text{ d}^{-1}$; Fig. 4).

Species composition in the top 15 m, from the hose sampling, indicated on 14 March a dominance of diatom biomass by *Skeletonema costatum* and *Chaetoceros* spp., with some pennate diatoms also contributing, but phytoplankton carbon was dominated by the larger *Coscinodiscus* spp. (Fig. 5). The rogue flagellate *Chattonella* sp. dominated surface biomass between 16 March and 23 March, except on the day of peak upwelling, when surface waters were displaced with subsurface water apparently containing primarily diatoms. Dinoflagellates, primarily heterotrophs, dominated cell numbers and cell carbon after the disappearance of *Chattonella* sp. through the remainder of the study (Fig. 5). Diatom carbon contributed 15–80% of the biomass during the first half of the study, and about 5% during the latter half. Interestingly, the large species *Coscinodiscus concinnus* and *C. centralis* contributed measurable amounts of diatom biomass throughout the study, and when the smaller species declined, these large cells remained to contribute almost 100% of the diatom carbon by the end of the study. Between 19 and 30 March, temporally integrated diatom carbon was 50% that of *Chattonella* sp.

Organic matter pools—Increases in POC and PON largely followed the same pattern as Chl *a* (Fig. 2C–D), with peak values ($>1000 \mu\text{g L}^{-1}$, = $83 \mu\text{mol L}^{-1}$) occurring both pre- and postupwelling at the surface. Both POC and PON showed the same subsurface peak at 20 m on 31 March as was seen in the Chl *a* signature, suggestive of phytoplankton sedimentation. Integrated POC inventories (0–15 m) showed a consistent increase across the time series, peaking at ~ 10

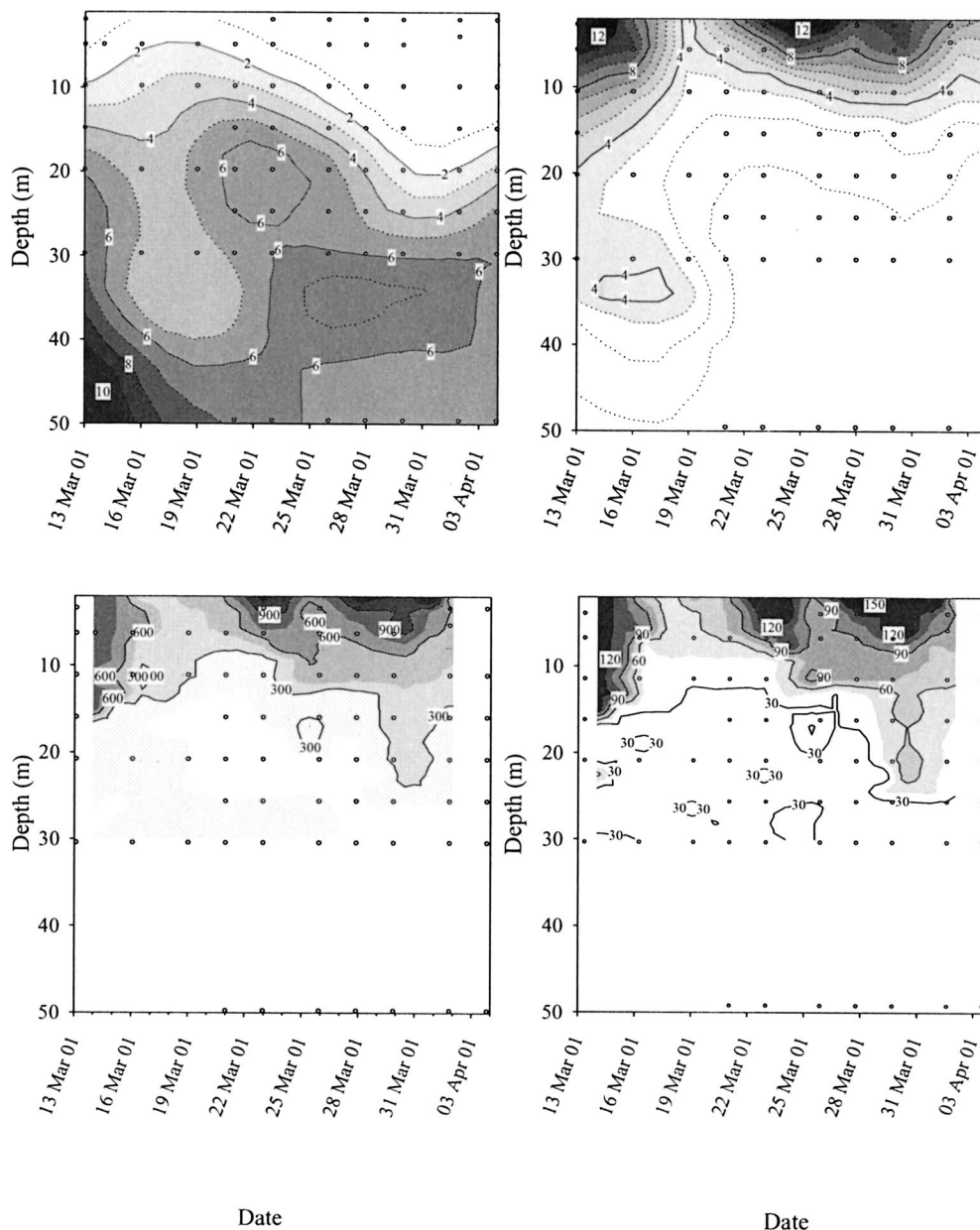


Fig. 2. Concentrations of key biogeochemical variables of interest with depth and time over the study period. Sampling dates and times are indicated as small circles. (A) Dissolved nitrate concentrations ($\mu\text{mol L}^{-1}$). Note depletion of nitrate to undetectable values to ~ 20 m by 30 March 2001. (B) Chl *a* concentrations. Note the >30 m peak on 16 March 2001, which contains sedimented biomass from the previous week's bloom of *Skeletonema costatum*. The strong surface peaks represent the intense bloom of the toxic flagellate *Chattonella* sp., which dominated surface waters during the early period of the study. (C) POC and (D) PON, both in $\mu\text{g L}^{-1}$. Most of the large peak of POC in surface waters is nonsinking and has a light -26‰ $\delta^{13}\text{C}$ signature, whereas the clearly visible sedimentation event around March 30 contains a heavier $\delta^{13}\text{C}$ signature (see Fig. 7).

g C m^{-2} on 30 March and declining thereafter (Fig. 6). Inventories integrated to 30 m reached 15 g C m^{-2} and showed a similar trend (Fig. 6). Other carbon components also had surface peaks. TEP concentrations decayed exponentially with depth and had a strong correlation with POC and PON overall, except that there was a strong peak in TEP accumulation at 5 m on 28 March (Fig. 7). DOC reached concentrations between 250 and $350 \mu\text{mol L}^{-1}$ at 5 m after 21 March, increasing from $200 \mu\text{mol L}^{-1}$ earlier in the study.

(This represented more than 300% of the carbon found in the form of POC.) A basic carbon inventory is shown in Table 1; estimates of phytoplankton carbon standing stock suggested that live biomass represented $\sim 10\%$ of total POC.

$\delta^{13}\text{C}$ signature of water column carbon—The most notable pattern in the profile of particulate material $\delta^{13}\text{C}$ was the very light $\delta^{13}\text{C}$ signature in surface waters ($< -26\text{‰}$), which was reasonably constant throughout the study period (19

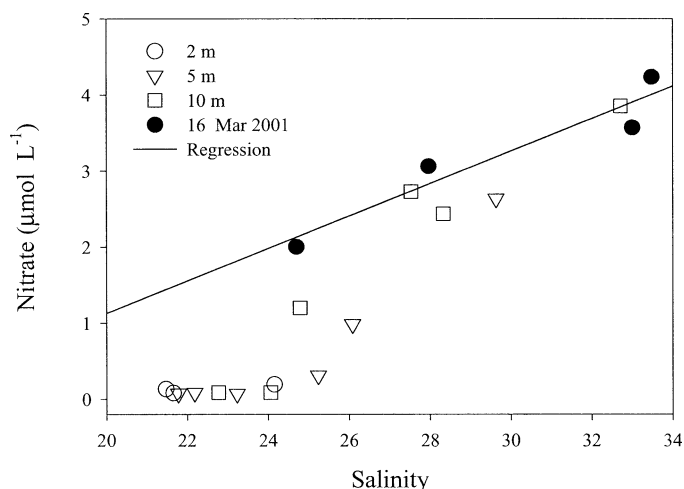


Fig. 3. Nitrate plotted versus salinity to differentiate between two possible loss factors for nitrate after 19 March 2001: upwelling relaxation and biological uptake. Decreases in nitrate concentration correlated with a decrease in salinity (the linear relationship is determined just before the peak upwelling 16 May 2001) are assumed to indicate dilution losses from the relaxation of the upwelling. Nonconservative losses of nitrate at a single salinity must be due to other factors such as biological uptake.

March to 30 March; Fig. 8) and did not move from the surface layer. Because of the large amount of DOC and TEP carbon with a surface peak, carbon in the moderate to small size fractions was a prime candidate as a source of this material. A heavy $\delta^{13}\text{C}$ signature (-22 to -19‰) was also visible as a pulse of material (Fig. 8) moving from the surface to depth over the period of the study. Based on the $\delta^{13}\text{C}$ signature, then, there were at least two distinct fractions of particulate organic matter—a nonsinking, low- $\delta^{13}\text{C}$ fraction, and a sinking, high- $\delta^{13}\text{C}$ fraction.

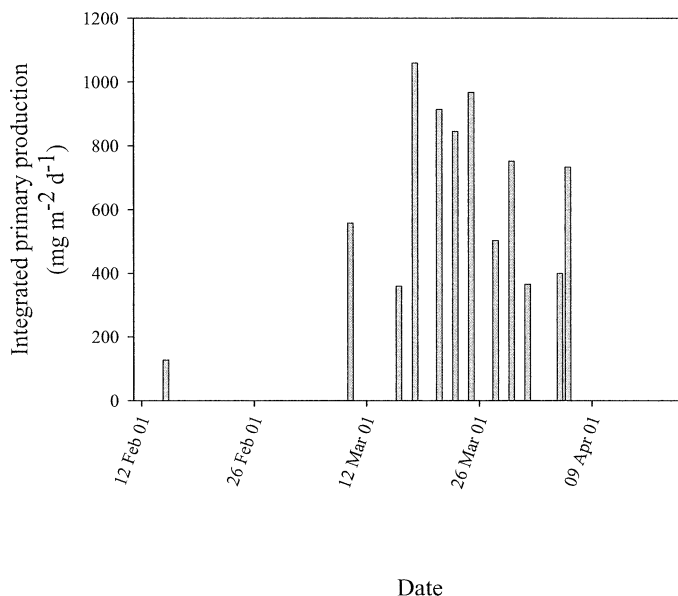


Fig. 4. Depth-integrated (0–20 m) primary production ($\text{mg C m}^{-2} \text{d}^{-1}$) versus time over the period of the study.

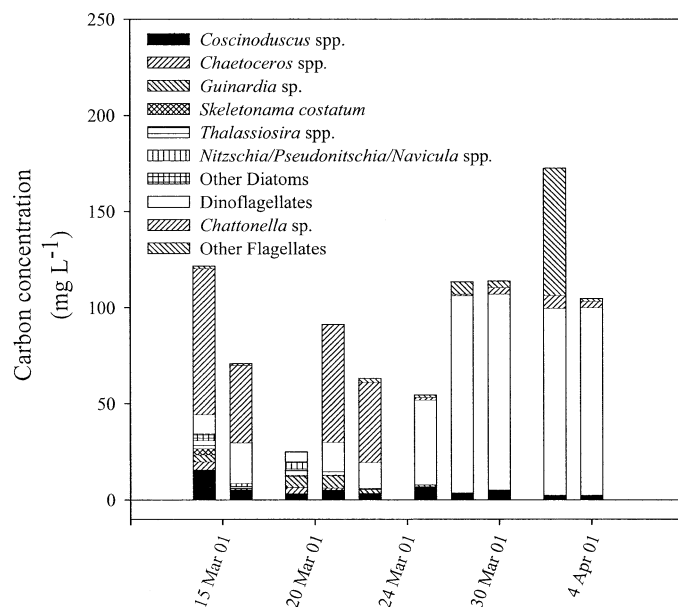


Fig. 5. Phytoplankton cell carbon ($\mu\text{g L}^{-1}$) estimated from cell numbers averaged over the top 15 m using a hose sampler. For each species or species group, the total carbon contribution was estimated using cell counts multiplied by cell carbon estimates from Edler (1977). Note that the large biomass of dinoflagellates in the latter half of the study is actually heterotrophic.

Sinking rates of various biogeochemical fractions—Bulk mean sinking rates from homogeneous sample SETCOL experiments indicated that bulk Chl *a* sinking rates were low (0 to 0.4 m d^{-1} ; Fig. 9A) and regularly showed significant ascent rates (Fig. 9B). Sinking rates of PON (measured 26 March onward) were significantly correlated ($p < 0.05$) with Chl *a* sinking rates, but were generally four to six times higher than those of Chl *a* (Fig. 9A). PON also showed significant ascent rates (up to 0.2 m d^{-1}), though not as high

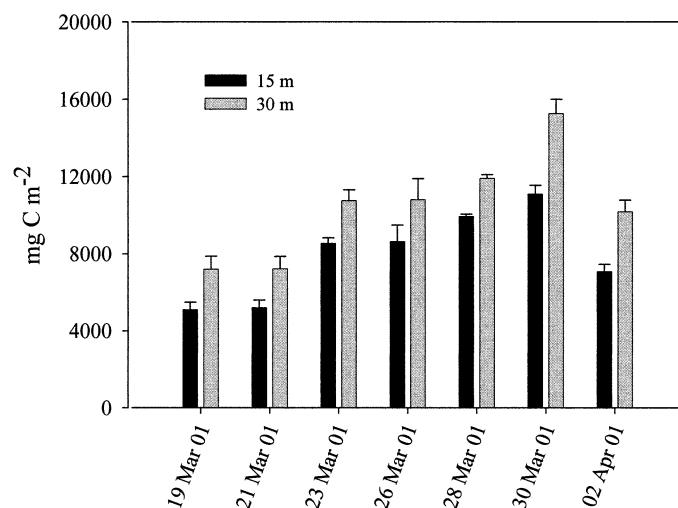


Fig. 6. Particulate organic carbon inventories (mg C m^{-2}) integrated to 15 m (black bars) and 30 m (gray bars). POC inventories increased with time and peaked on 30 March 2001, when the maximum sedimentation event occurred.

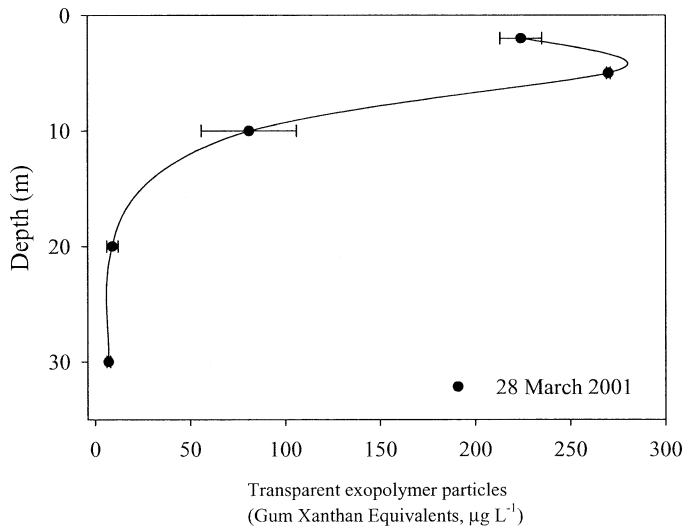


Fig. 7. Profile of TEP concentrations on 28 March 2001, when TEP peaked at 5 m. TEP values were highest in near surface waters throughout the study.

as the ascent rates of Chl *a* (Fig. 9B). Ascent rates are generally seen when cells are in excellent physiological condition and are large enough that their internal vacuole buoyancy can outcompete the ballast of the silica frustule (Waite et al. 1992b). POC sinking rates were higher still and showed no significant correlation with either PON or Chl *a* sinking rates (Fig. 9A). We measured no significant ascent rate for POC at any time during the study (Fig. 9B). When the chemical composition of the material in the three SETCOL fractions for the POC and PON experiments was compared, the bottom fraction was significantly ($p < 0.05$) different than the top and middle fractions, which were similar to each other (Fig. 10A–B). The $\delta^{13}\text{C}$ of the rapidly sinking fractions was significantly heavier, and the POC:PON molar ratios were significantly higher, than the more slowly sinking fractions (Fig. 10A–B).

In all layered sinking fractionation experiments with sink-

ing rate cutoffs, material with a heavier (less negative) carbon isotope signature sank more quickly than bulk material (Table 2). However, the isotope fractionation showed markedly different results depending on the source material. The net hauls $>90 \mu\text{m}$ on 26 and 28 March had a mean $\delta^{13}\text{C}$ of -18.5 to -19.9‰ for the two net hauls, respectively, whereas the bulk $>0.22 \mu\text{m}$ sample had a mean $\delta^{13}\text{C}$ of -26‰ (Table 2). When examined under the microscope, the net haul material consisted almost entirely ($>99\%$) of large diatoms of the species *C. concinnus* and *C. centralis*. This gave a useful estimate of the $\delta^{13}\text{C}$ of pure diatom material. Sinking fractionation within this highly uniform sample was still apparent, with the bottom fractions again showing heavier $\delta^{13}\text{C}$ values (-18.5 and -19.9‰) and the top fractions showing lighter values (-23.5 and -20‰). Eighty-three percent to 92% of the POC and 82–83% of the PON sank faster than 1 m d^{-1} in these samples, whereas less than 1% of these samples did not sink over the experiment period (12 h). In the $>0.22 \mu\text{m}$ sample, only 2.3% of the POC and 15.5% of the PON sank faster than 1 m d^{-1} , whereas 18.4% of the POC and 16.6% of the PON did not sink. There was a change in $\delta^{13}\text{C}$ of $\sim 2\text{‰}$ between the top (not sinking) and the bottom (sinking $>1 \text{ m d}^{-1}$) fractions. The $>1 \text{ m d}^{-1}$ fraction had a $\delta^{13}\text{C}$ signature of -23.8‰ (Table 2). Differential remineralization within the columns, as well as differential sinking, could be a factor driving the vertical change in signature within the columns. However, there was no loss of POC during the SETCOL experiments, as evidenced by there being no change in the additive POC fractions compared with the original samples. This suggests that there was no measurable loss of carbon via remineralization, and that differential sinking was the primary factor driving the observed vertical gradient.

Colloid flocculation experiment—The colloid flocculation experiment indicated that COC in $<0.22 \mu\text{m}$ filtered seawater coagulated to yield measurable GF/F filterable POC (i.e., $>0.7 \mu\text{m}$) when flocculated at 5 s^{-1} for as little as 1 h (Fig. 11A). No significant further coagulation was observed

Table 1. Integrated standing stock inventories (mg C m^{-2} , or mg other compound m^{-2} where indicated) and integrated production estimates ($\text{mg C m}^{-2} \text{ d}^{-1}$, or $\text{mg Chl } a \text{ m}^{-2} \text{ d}^{-1}$ where indicated) during the period of constant water mass (19 Mar through 30 Mar 2001).

	Standing stock	Water column production rates/Trap fluxes	
	Integrated peak carbon to 30 m (mg C m^{-2})	Peak production/Flux to sediment traps ($\text{mg C m}^{-2} \text{ d}^{-1}$)	Integrated production/Flux to sediment traps (mg C m^{-2})
Primary production (^{14}C uptake 0–20 m)		30 ($\text{mg C m}^{-3} \text{ d}^{-1}$)	4,300
New production		1,000	2,970
Particulate organic carbon (POC)	10,000–14,000	1,900	4,144
Transparent exopolymer particles	2,600 (mg GXE m^{-2})	25	71
Dissolved organic carbon (DOC)	36,000		
Chlorophyll <i>a</i>	120 ($\text{mg Chl } a \text{ m}^{-2}$)	13 ($\text{mg Chl } a \text{ m}^{-2} \text{ d}^{-1}$)	36 ($\text{mg Chl } a \text{ m}^{-2}$)
<i>Chattonella</i> sp.	615	9	13
Diatoms	300	90	196
<i>Coscinodiscus</i> spp.	105	69	131
Diatom exudate (POC)			$\sim 3,851$
Fecal pellets		6.4	53

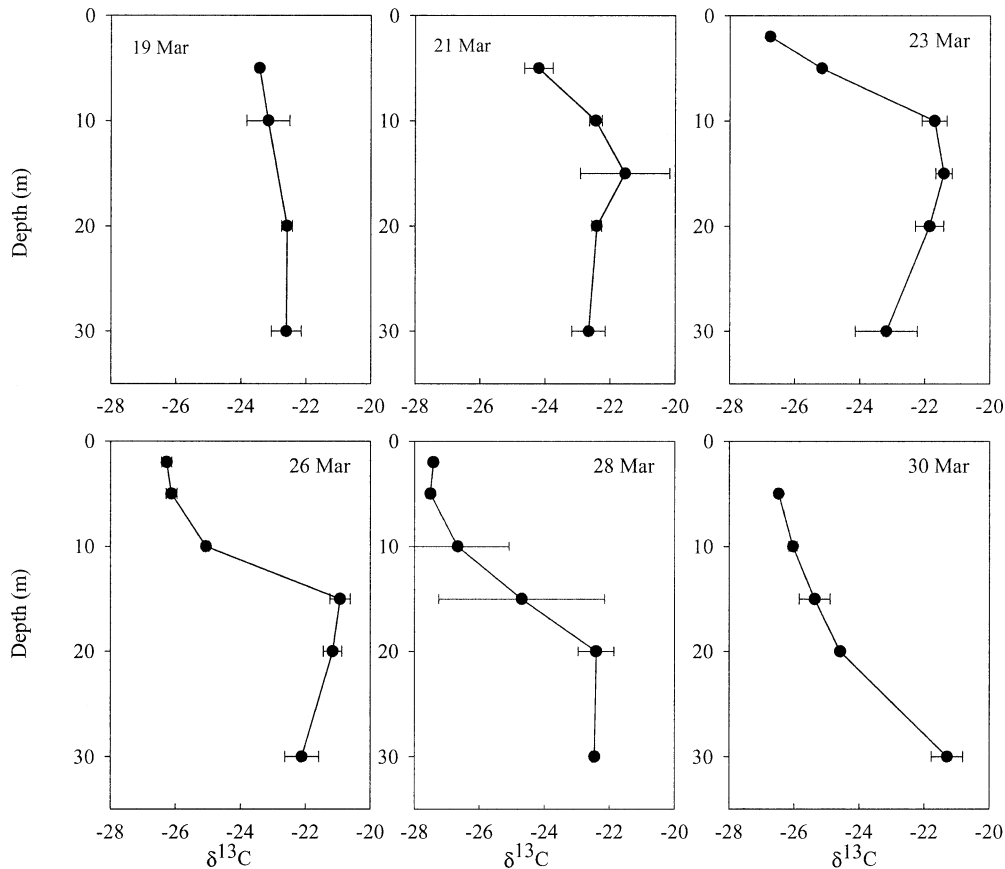


Fig. 8. $\delta^{13}\text{C}$ profiles of filterable POC between 19 March and 30 March 2001. Note the light signature (-26‰) near the surface and the heavier signature at depth, forming a sinking peak to 30 March 2001 (-21 to -22‰). Error bars represent standard deviations of duplicate analyses.

with flocculation for up to 9 h. A contemporaneous shift in the $\delta^{13}\text{C}$ signature of filterable POC to extremely low values ($< -32\text{‰}$) indicated that this colloidal material moving into the POC during flocculation had a significantly lighter $\delta^{13}\text{C}$ signature than bulk POC (Fig. 11B). Although only 2.9% of the DOC flocculated, because of the large DOC pool, 2.9% amounts to 70 mg m^{-3} , or 2.1 g m^{-2} when integrated over 30 m. This represents $2\times$ daily integrated primary production, $6\times$ the integrated diatom biomass, and $\sim 20\%$ of the POC standing stock.

Sediment trap flux—The time series of POC flux to the sediment traps indicates that there was a major sedimentation event 28–30 March. The POC sedimentation peak occurred at 15 m between 26–28 March ($\sim 2.5\text{ g C m}^{-2}\text{ d}^{-1}$) and 30 m between 26–30 March ($1.9\text{ g C m}^{-2}\text{ d}^{-1}$) (Fig. 12A), the latter representing 44% of the integrated primary production over the period and $\sim 63\%$ of the carbon available for export (new production) according to the estimated NO_3 drawdown over the period (Fig. 3; Table 1). However, based on cell carbon estimates, whole live cells could account for $< 90\text{ mg m}^{-2}\text{ d}^{-1}$, only about 4% of the total sedimenting carbon for this 28–30 March period (Fig. 12B). Amorphous POC measured as TEP could account for up to $25\text{ mg m}^{-2}\text{ d}^{-1}$, or 1% (as Gum Xanthan Equivalents [GXE]) reaching the sediment traps (Gustafsson et al. unpubl. data). Fecal pellets accounted

for $6.39\text{ mg m}^{-2}\text{ d}^{-1}$. However, the $\delta^{13}\text{C}$ signature of the material in the sediment traps was -18.5 to -21.5‰ (Fig. 12C), which is identical to the range found in the net haul containing almost pure diatom material (Table 2). Observation of material in the sediment traps indicated that the phytoplankton fraction of this sedimentation peak was indeed dominated by diatoms, primarily *Coscinodiscus* spp. (Fig. 13A–B).

Sediment trap gel images indicated a change in the quality of the sedimented material over time (Fig. 13A–B). Small organic particles and solitary diatom cells and chains dominated early samples (19 March, Fig. 13A), whereas larger and more complex aggregate particles formed later in the sedimentation event (Fig. 13B). *Coscinodiscus* spp. was visible in all trap gels, but in later samples were more abundant and always embedded in an organic matrix. This matrix, visible as amorphous yellow-brown material between cells, became more evident and extensive between cells over the time series.

Discussion

Our analysis follows the growth and sedimentation of a complex secondary phytoplankton bloom in the Gullmar Fjord, Sweden, in spring 2001. The fjord represents a typical coastal temperate ecosystem, which has been studied for

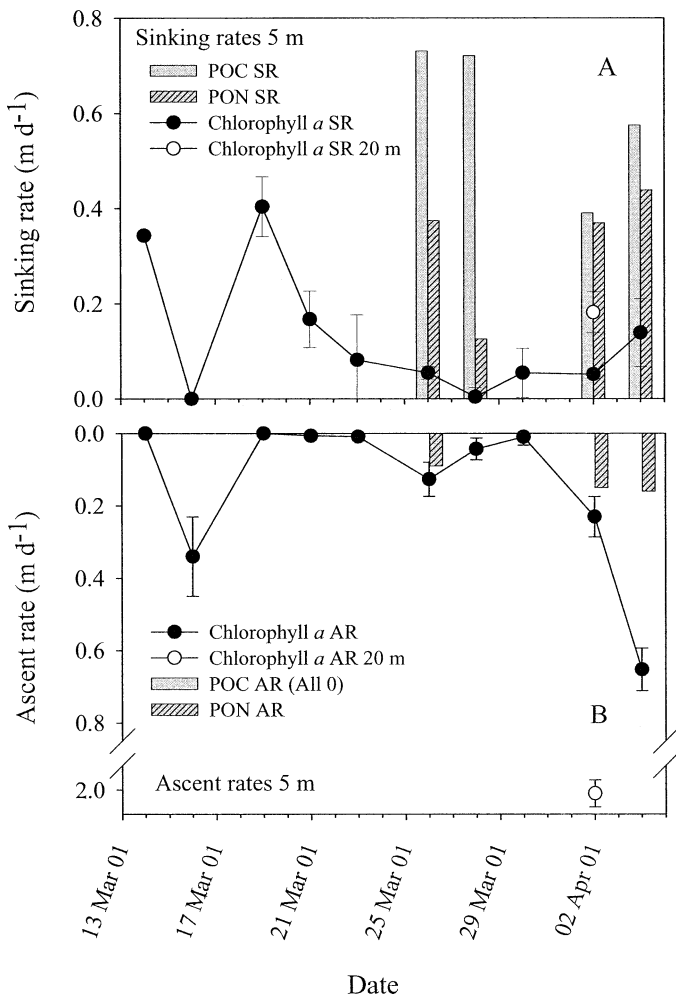


Fig. 9. Time series of bulk SETCOL sinking and ascent rates of different fractions of particulate organic matter in surface waters. (A) Mean Chl *a* sinking rates are indicated as filled circles; a single measurement from 20 m on 25 March 2001 is also indicated. Error bars indicate standard deviation of triplicate columns. POC and PON sinking rates (measured four times, only after 25 March 2001) are shown as single bars, each representing an individual measurement. (B) Mean ascent rates, all else as in panel A.

over 20 years (Lindahl 1983). Diatoms are a dominant feature of fjord ecology (McQuoid 2002) and can contribute significantly to carbon sedimentation (Tiselius and Kuylenstierna 1996). However, abundant dinoflagellate populations bloom under conditions of suitable temperature and salinity (Godhe et al. 2001). In addition, a large and varied population of secondary and tertiary grazers has been documented, whose dynamics can dominate entirely the ecology of the fjord (Graneli and Turner 2002).

Here, we investigate the primary pathways by which carbon is moved through the Gullmar Fjord ecosystem in the spring. Despite the dominance of heterotrophic and autotrophic flagellates in surface waters both in terms of cell numbers and carbon throughout the bloom, the large diatoms growing at modest background concentrations carried most of the carbon flux, and a distinctive carbon isotope signature, to depth. We explore the functional separation between the

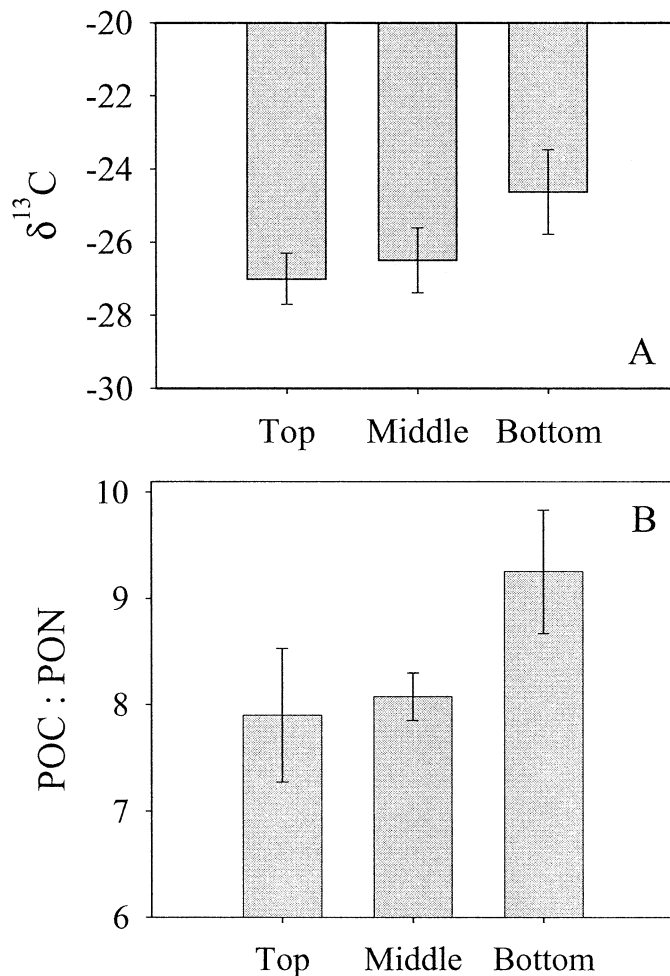


Fig. 10. (A) Carbon isotope signatures ($\delta^{13}\text{C}$, in ‰) in the top, middle, and bottom fractions of the POC and PON SETCOL sinking experiments. These fractions are biased toward rapidly ascending, neutrally buoyant, and rapidly sinking particles, respectively. Error bars indicate standard deviation between the four experiments. (B) POC:PON molar ratio in top, middle, and bottom fractions of the SETCOL, as for panel A.

sinking and nonsinking fractions of this ecosystem, and the geochemical consequences of what we term “sinking fractionation.”

Productivity levels were typical of those found in the fjord at this time of year, based on a comparison with long-term datasets (Lindahl 1995). The toxic flagellate *Chattonella* sp. dominated the surface phytoplankton community in the early part of our study, contributing $\sim 1 \text{ g C m}^{-2}$ to total integrated productivity over the study period (Waite and Lindahl unpubl. data), and was possibly consumed by a large population of heterotrophic dinoflagellates, respired, and/or possibly exuded as dissolved organic carbon in surface waters (Waite and Lindahl unpubl. data). Thus, we envisage that most of the *Chattonella* sp. bloom carbon eventually contributed to the pool of dissolved, colloidal, and particulate carbon remaining suspended in the water column.

A significant population of diatoms coexisted with the *Chattonella* sp. bloom. Because of their higher sinking rates,

Table 2. Percent (by weight) of organic carbon (POC) and nitrogen (PON) sinking at 0 m d⁻¹, between 0 and 1 m d⁻¹, and above 1 m d⁻¹, and $\delta^{13}\text{C}$ of each fraction, in samples concentrated (A) $>0.22\ \mu\text{m}$ ($n = 1$) and (B) $>90\ \mu\text{m}$ (via net haul) ($n = 2$).

Experiment/ sample fraction	% C in column fraction	$\delta^{13}\text{C}$	% N in column fraction
(A) 0.22 μm Retentate			
27 Mar 2001			
Not sinking	18.4	-25.5	16.6
Sinking 0–1 m d ⁻¹	79.4	-26.2	67.9
Sinking >1 m d ⁻¹	2.23	-23.8	15.5
Total	100	-26.0	100
(B) Net haul >90 μm			
26 Mar 2001			
Not sinking	0.70	-20.0	1.33
Sinking 0–1 m d ⁻¹	7.21	-20.2	15.4
Sinking >1 m d ⁻¹	92.1	-19.9	83.2
Total	100	-19.9	100
28 Mar 2001			
Not sinking	0.73	-23.5	1.43
Sinking 0–1 m d ⁻¹	15.83	-18.4	15.0
Sinking >1 m d ⁻¹	83.4	-18.5	83.6
Total	100	-18.5	100

diatoms were primary candidates for the contribution to the sedimentation event later in the study. In this case, we look to the $\delta^{13}\text{C}$ signature in the water column and the fractionation of this signature in laboratory sinking experiments to clarify the chemical contributions of various ecosystem components to the vertical flux. The isotopic signature of various ecosystem components (Rolff 2000; Lorrain et al. 2002; Riera et al. 2002) and other chemical tracers of ecosystem components, such as algal pigments (Bianchi et al. 1997), are increasingly being used to analyze the structure and function of ecosystems.

Two primary features of the $\delta^{13}\text{C}$ signature were of interest: the low $\delta^{13}\text{C}$ of surface waters (-26 to -28‰) and the higher $\delta^{13}\text{C}$ signal forming a sinking peak (-21 to -20‰). The very low $\delta^{13}\text{C}$ signature seen in POC from surface waters is typical of small ($<10\ \mu\text{m}$) POC and DOC in spring to early summer in Baltic surface waters (Rolff 2000). The moderately low signatures at 30 m depth (-22 to -25‰) could possibly be associated with larger, grazing populations, i.e., carbon from higher trophic levels (Rolff 2000), but large grazers were not abundant. In our study, the surface $\delta^{13}\text{C}$ signature was high on the day of peak upwelling; anecdotally, these deeper waters were also rich in diatoms and contained almost no *Chattonella* biomass. Given that surface POC concentrations were 10 times greater than our estimates of phytoplankton carbon and heterotrophic dinoflagellate carbon, the dominance of the signal by components of the microbial loop seemed likely, including microbial biomass and nonliving POC relic from past microheterotrophic activity. We also hypothesize a possible contribution by heterotrophic grazers targeting the surface *Chattonella* sp. bloom.

The pool of carbon in surface waters was measured as POC (particles $>0.7\ \mu\text{m}$), and as dissolved/colloidal organic

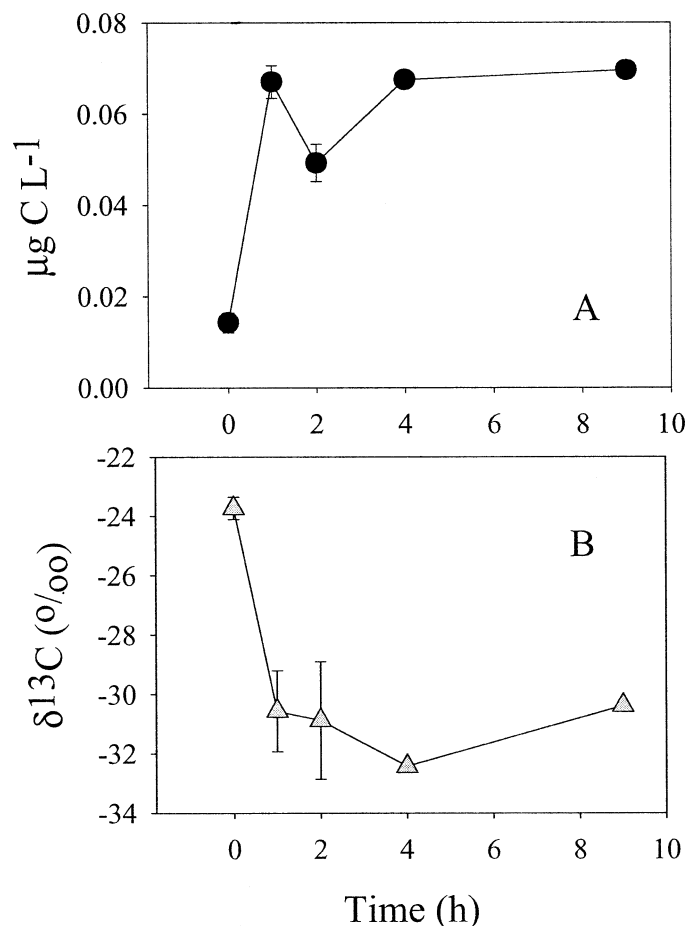


Fig. 11. (A) Colloid flocculation experiment from 5 m surface water indicating that filterable COC ($<0.22\ \mu\text{m}$) can aggregate to form filterable POC ($>0.7\ \mu\text{m}$) after as little as an hour under a shear of $5\ \text{s}^{-1}$. (B) The resulting filterable POC has an extremely low $\delta^{13}\text{C}$ (-32‰), which could be a significant contributor to the low $\delta^{13}\text{C}$ signature in nonsinking material in surface waters. Error bars indicate standard deviation of two replicate flocculation experiments over the same time frame.

carbon (DOC/COC, $<0.22\ \mu\text{m}$), some of which was also measured independently as TEP, which would include small POC and some filterable COC. Definitions of these fractions can vary (e.g., Gustafsson and Geschwend 1997), but all organic C fractions showed a strong surface peak (DOC and COC ~ 2 times POC), again suggesting that they would have dominated the $\delta^{13}\text{C}$ signal. The colloid aggregation experiment showed conclusively that some of the massive carbon pool in dissolved/colloidal ($<0.22\ \mu\text{m}$) size fraction could aggregate to POC ($>0.7\ \mu\text{m}$), and this fraction had an extremely light $\delta^{13}\text{C}$ (-31 to -32‰), significantly lower than those measured by other investigators (Rolff 2000). However, sinking experiments seemed to suggest that this light carbon fraction seemed to remain primarily in suspension rather than sinking: filterable nonsinking particles had lower $\delta^{13}\text{C}$ by about 3–7‰ than their sinking counterparts. The nonsinking fraction would have included nonsinking phytoplankton, microheterotrophs, and nonliving POC with a low or negligible sinking rate. Overall, the non-

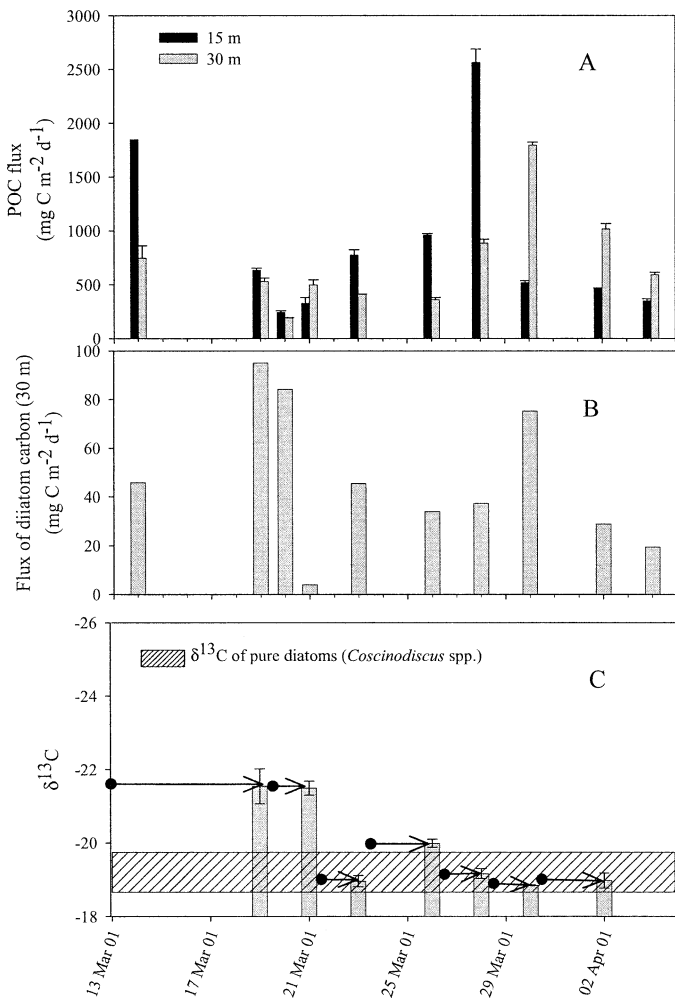


Fig. 12. Characteristics of POC flux to sediment traps moored at 15 m and 30 m in the fjord. (A) Temporal POC flux ($\text{mg C m}^{-2} \text{d}^{-1}$) to 15 m and 30 m. Peak POC flux occurred on 28 March 2001 at 15 m and on 30 March 2001 at 30 m. Error bars indicate standard deviation of two replicate sediment traps. (B) Flux of diatom carbon (intact whole cells) calculated from cell counts multiplied by carbon contents of individual species as estimated by Edler (1977). (C) $\delta^{13}\text{C}$ of total flux to 30 m sediment traps. The characteristic $\delta^{13}\text{C}$ of *Coscinodiscus* sp. from the 90-mm net hauls on 26 March and 28 March 2001 are included for comparison purposes. Arrows indicate duration of sediment trap deployments.

living and nonsinking small POC and COC are the most likely contributors to the low $\delta^{13}\text{C}$ found in surface waters, with some contribution from microheterotrophs. The separation of the carbon pool into sinking and nonsinking components with very different $\delta^{13}\text{C}$ in our experiments might be considered a type of "sinking fractionation" of the carbon isotope signal, where biologically determined processes cause a physical, rather than a biological, separation of the carbon isotope signal. This might have significant implications for paleo-reconstructions of past ecosystems from $\delta^{13}\text{C}$ in the sedimentary record (Lee et al. 1987; Burkhardt et al. 1999).

Sinking rates of different analytical fractions of particulate material in bulk sinking rate experiments (e.g., Chl *a*, PON,

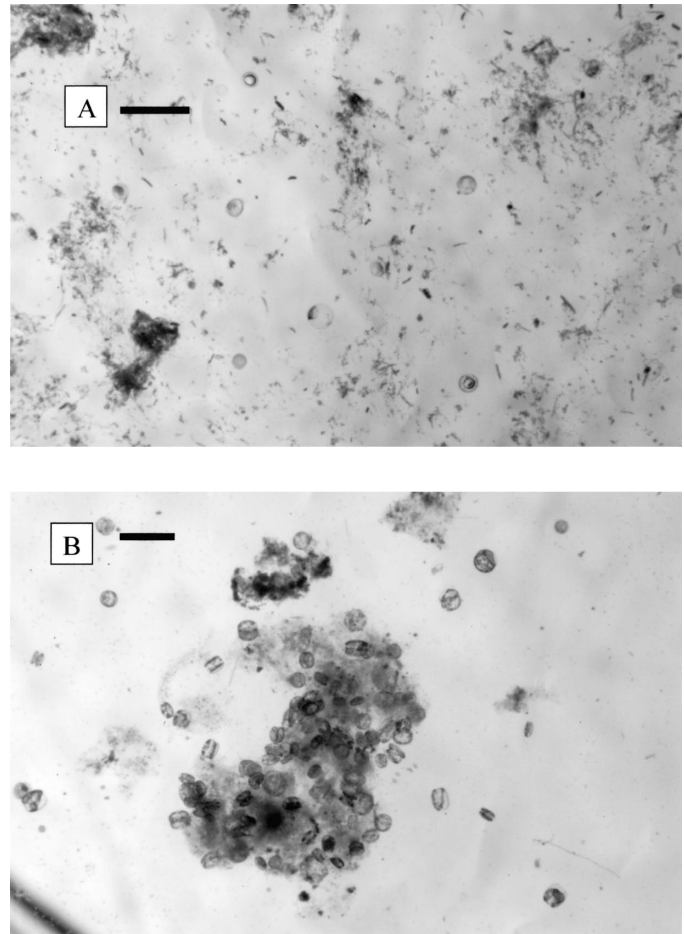


Fig. 13. Images of particles in the sediment traps as collected in sediment trap gels (A) early in the study (19 March 2001) and (B) at the peak of the sedimentation event on 30 March 2001. Scale bar = 1 mm.

and POC in SETCOL analyses) give an indication that particles containing high concentrations of each of these materials have differences in sinking rates (Waite et al. 1992a). For example, the consistently low sinking rates of Chl *a* throughout the study indicate that phytoplankton with high Chl *a* concentrations (in general, rapidly growing healthy cells) tend to have low sinking rates and measurable ascent rates (Waite et al., 1992b). The correlation between Chl *a* and PON sinking rates suggests that these fractions may occur in similar or associated particles, probably a combination of phytoplankton and some microheterotrophs. The low sinking rates of Chl *a* and PON in comparison to POC throughout the study suggest that on the whole, such live cells sink very slowly in comparison to bulk organic carbon, which must therefore be sinking, on average, packaged in particles containing a low Chl *a*:POC ratio. In fact, the dissimilarity between patterns of POC sinking rates versus PON and Chl *a* sinking rates suggests that they are virtually moving as separate pools.

The most rapidly sinking carbon fraction in the sinking experiments and bulk SETCOLs always had the highest $\delta^{13}\text{C}$ of the sample. This was true even in the most extreme case

of the isolated population of large ($>90 \mu\text{m}$) *C. centralis* and *C. concinnus* cells, which had overall the highest $\delta^{13}\text{C}$ of all fractions measured (-19 to -21‰). The dominance of large diatom species may partially explain the unusually heavy (i.e., relatively unfractionated) isotopic signatures of the diatom carbon found in our study. The $\delta^{13}\text{C}$ of diatoms is driven primarily by the strong fractionation of the carbon-fixing enzyme RUBISCO, but is affected by cell size, ambient dissolved inorganic carbon concentrations, and a number of environmental factors affecting growth rates (Popp et al. 1998; Burkhardt et al. 1999). A related species, *Coscinodiscus walesii*, has been shown to cause less fractionation than other diatoms, possibly related to its large size (Burkhardt et al. 1999).

This heavy diatom $\delta^{13}\text{C}$ signature also moved as a sedimenting peak through the POC profile, identifying the large diatoms as the primary contributors to the sinking layer and to sinking fractionation within the fjord. As detailed elsewhere (Waite and Lindahl unpubl. data), it is likely that the nonsinking autotrophic carbon was grazed, and thus respired and/or lost as DOC during feeding. In the long term, we expect that this material would accumulate the very light $\delta^{13}\text{C}$ typical of that found in surface waters of the fjord.

Sediment trap cell counts indicated that the major carbon sedimentation event was driven almost entirely by large numbers of the largest diatoms, *Coscinodiscus* spp., with a small contribution from other diatoms. Single cells and chains made a significant contribution to the flux only early in the study. The visible dominance of aggregated particles in the sediment trap gels suggested that much of the rapid sedimentation event was driven by aggregation of *Coscinodiscus* spp. and other diatoms into larger sinking particles. Quantitatively, the majority of the sedimented carbon could not be accounted for by live cells or by fecal pellets. The large amount of amorphous material between cells in the aggregates was the single most visible component in the gels, and is likely to be the primary contributor to carbon flux. It was therefore of interest to determine the origin of this material, which may among other roles have played a key role in sedimentation by contributing to cell stickiness and aggregation.

The large pool of POC, COC, and/or TEP in surface waters seemed to be a prime candidate for this material, because our aggregation experiment showed that this material could aggregate into filterable particles. Studies in freshwater have shown that such processes are not scale specific, such that subcolloidal material can aggregate into colloids, and colloids into microparticles, under Brownian motion alone (Kerner et al. 2003). Only a small fraction of the large surface carbon pool, if it aggregated with sinking diatoms, could easily account for the observed carbon flux. As discussed above, the $\delta^{13}\text{C}$ of this surface DOC, COC, and/or TEP pool is distinctively light ($\sim 32\text{‰}$ for material freshly aggregated from subcolloids and colloids in our experiment, different from the freshwater case, where aggregating colloids were shown to have a heavier $\delta^{13}\text{C}$ [-20 to -23] than bulk material [Kerner et al. 2003]), and should be identifiable via its isotope signal in the sedimented material if it provides the majority of the carbon flux.

However, the $\delta^{13}\text{C}$ of the sedimented material was actually

very heavy during the primary sedimentation event on 30 March (-19‰), identical to that of the fresh diatom biomass. This excludes the possibility that aggregating surface COC is the primary source of the material and suggests that the amorphous sedimented material visible in the aggregates is in fact a type of exudate of recent diatom origin. Diatoms are known to exude 10–60% of the carbon they fix (Bjornsen 1988), as DOC, surface-associated simple sugars, and TEP (Waite et al. 1995). In this case, the TEP budget indicated that only a small fraction of the TEP produced in surface waters was measured in the sediment traps (Gustafsson et al. unpubl. data). So it seems in this case that non-TEP polymers, relatively freshly exuded from rapidly growing diatom cells, and remaining associated with the cells in increasingly large aggregates, were the single greatest contributors to the carbon flux of the Gullmar Fjord during this period. This sedimented POC of diatom origin could account for $\sim 150\%$ of the new production as estimated by nitrate drawdown in surface waters, and 75–80% of total primary production measured experimentally over the period. On the basis of integrated primary production estimates of $\sim 4.3 \text{ g C m}^{-2}$ and *Chattonella* sp. production of $\sim 1 \text{ g C m}^{-2}$, it is likely that diatoms were therefore responsible for temporally and depth-integrated production of just over 3 g C m^{-2} over the period of the study. It is worth noting that this diatom-derived carbon dominated the vertical flux despite the fact that diatom cells represented only 30% of the biomass-associated POC in surface waters.

The heavy isotopic composition of this material contrasts with work of investigators working in freshwater who found diatom exudates with a $\delta^{13}\text{C}$ of -42‰ , consistent with strong fractionation within the phytoplankton (Kerner et al. 2003). However, van Dongen et al. (2002) made detailed characterization of the $\delta^{13}\text{C}$ of monosaccharides in several phytoplankton and suggest that simple sugars in phytoplankton are generally enriched in ^{13}C relative to bulk cells (by 1–16‰). This would suggest the possibility that the diatoms are exuding such enriched components, consistent with work by Waite et al. (1995), who used lectin labeling to show that a number of diatom species exude glucose- and mannose-rich compounds in log phase growth. These accumulated in batch media to peak concentrations in early stationary phase, and were associated with a significant increase in stickiness leading to aggregation (Waite et al. 1997a). It is possible that the exudate material is released from the diatoms from the monosaccharide pool before significant fractionation occurs, possibly at the stage of primary carbon chain formation.

Interestingly, the $\delta^{13}\text{C}$ of the sediment trap material was more negative early on in our study, possibly suggesting a measurable input from light $\delta^{13}\text{C}$ sources. Because TEP and fecal pellets made minimal contributions to the sediment trap fluxes (see Table 1), we might assume that this light component originated as surface COC with a $\delta^{13}\text{C}$ of -32‰ . Assuming two primary components of the POC are diatom carbon with a $\delta^{13}\text{C}$ of -18 to -19‰ , and aggregated surface COC with a $\delta^{13}\text{C}$ of -32‰ , then the signature of -21.5‰ of the sedimented material between 13 and 19 March would indicate that approximately 23% of the sediment trap material on those dates had its origin as COC, suggesting that

some of this highly fractionated carbon can in fact contribute to sedimentation fluxes under certain conditions. With only $\sim 90 \text{ mg m}^{-2} \text{ d}^{-1}$ attributable to whole diatom cell flux, the remainder of diatom carbon (some $319 \text{ mg m}^{-2} \text{ d}^{-1}$) is highly likely to be diatom cell exudates (60% of the total POC flux between 13 and 19 March).

If we also reinterpret the surface water POC isotope signal as a combination of these two primary carbon sources, this suggests that 42% of surface POC was of recent diatom/phytoplankton origin, and 58% was aggregated COC and/or microbial loop components.

Overall, sinking fractionation caused shifts in the $\delta^{13}\text{C}$ (enrichment of 3 to 7‰) equal to or greater in magnitude than those seen by grazing in other studies (depletion by 0.3–4‰; Rolff 2000). The highly enriched sediment trap $\delta^{13}\text{C}$ indicated the dominance of diatom carbon in the flux, possibly explaining trends in other studies in which the sedimented $\delta^{13}\text{C}$ was lower than that in the water column, and peak $\delta^{13}\text{C}$ values were associated with phytoplankton sedimentation (Rolff 2000).

Here, we identify the process of sinking fractionation, as measured by differential sinking of components with varied carbon isotope signal, as an important process in determining carbon fluxes within a complex coastal ecosystem, the Gullmar Fjord, Sweden. Large, rapidly sinking diatoms aggregated with their own carbon exudates, which amounted to several times the live biomass. These diatoms carried to depth a heavy carbon isotope signature (–19‰) distinct from the nonsinking material. Sinking diatoms and diatom exudates represented 44% of integrated primary production, despite the fact that diatoms were at any one time only a trace component of integrated water column carbon. A large pool of colloidal carbon and small particulates typical of the microbial loop remained suspended in the water column with a lighter carbon isotope signature (–26‰), a component of which was the very low –32‰ of aggregating organic colloids.

References

- AXELMAN, J., AND Ö. GUSTAFSSON. 2002. Global sinks of PCBs: A critical assessment of the vapour-phase hydroxy radical sink emphasizing field diagnostics and model assumptions. *Global Biogeochem. Cycles* **16**: 1111–1124.
- BERGER, W. H., V. SMETACEK, AND G. WEFER. 1989. Ocean productivity and paleoproductivity—an overview, p. 1–34. *In* W. H. Berger, V. Smetacek, and G. Wefer [eds.], *Productivity of the ocean: Present and past*. Dahlem Workshop Reports. Wiley.
- BIANCHI, T. S., C. ROLFF, AND C. D. LAMBERT. 1997. Sources and composition of particulate organic carbon in the Baltic Sea: the use of plant pigments and lignin-phenols as biomarkers. *Mar. Ecol. Prog. Ser.* **156**: 25–31.
- BIENFANG, P. K. 1981. SETCOL: A technologically simple and reliable method to measure phytoplankton sinking rates. *Can. J. Fish. Aquat. Sci.* **38**: 1289–1294.
- BJORNSEN, P. K. 1988. Phytoplankton exudation of organic matter: Why do healthy cells do it? *Limnol. Oceanogr.* **33**: 151–154.
- BOTTRELL, H. H., AND D. B. ROBINS. 1984. Seasonal variations in length, dry weight carbon and nitrogen of *Calanus helgolandicus* from the Celtic Sea. *Mar. Ecol. Prog. Ser.* **14**: 259–268.
- BROMAN, D., C. NAF, J. AXELMAN, C. BANDH, H. PETTERSEN, R. JOHNSTONE, AND P. WALBERG. 1996. Significance of bacteria on marine waters for the distribution of hydrophobic organic contaminants. *Environ. Sci. Technol.* **30**: 1238–1241.
- BURKHARDT, S., U. RIEBESELL, AND I. ZONDERVAN. 1999. Effects of growth rate, CO_2 concentration, and cell size on the stable carbon isotope fractionation in marine phytoplankton. *Geochim. Cosmochim. Acta.* **63**: 3729–3741.
- CHIN, W.-C., M. V. ORELLANA, AND P. VERDUGO. 1998. Spontaneous assembly of marine dissolved organic matter into polymer gels. *Nature* **391**: 568–572.
- DAFNER, E. V., AND P. J. WANGERSKY. 2002. A brief overview of modern directions in marine DOC studies part II—recent progress in marine DOC studies. *J. Environ. Monit.* **4**: 55–69.
- DAVIS, C. S., S. M. GALLAGER, AND A. R. SOLOW. 1992. Microaggregations of oceanic plankton observed by towed video microscopy. *Science* **257**: 230–232.
- DONEY, S. C. 1999. Major challenges confronting biogeochemical modeling. *Global Biogeochem. Cycles* **13**: 705–714.
- EDLER, L. 1977. Phytoplankton and primary production in the Sound. Ph.D. thesis, Gothenburg University.
- GARDNER, W. D. 1997. Visibility in the ocean and the effects of mixing. *Quarterdeck* **5**: 4–9.
- GODHE, A., F. NOREN, M. KUYLENSTIERN, C. EKBERG, AND B. KARLSON. 2001. Relationship between planktonic dinoflagellate abundance, cysts recovered in sediment traps and environmental factors in the Gullmar Fjord, Sweden. *J. Plankton Res.* **23**: 923–938.
- GONZALEZ, H. E., AND V. SMETACEK. 1994. The possible role of the cyclopoid copepod *Oithona* in retarding vertical flux of zooplankton faecal material. *Mar. Ecol. Prog. Ser.* **113**: 233–246.
- GRANELI, E., AND J. T. TURNER. 2002. Top-down regulation in ctenophore-copepod-ciliate-diatom-phytoflagellate communities in coastal waters: A mesocosm study. *Mar. Ecol. Prog. Ser.* **239**: 57–68.
- GUSTAFSSON, Ö., AND P. GSCHWEND. 1997. Aquatic colloids: Concepts, definitions and current challenges. *Limnol. Oceanogr.* **42**: 519–528.
- GUSTAFSSON, A. DÜKER, J. LARSSON, P. ANDERSSON, AND J. INGRI. 2000. Functional separation of colloids and gravitoids in surface waters based on differential settling velocity: Coupled cross-flow filtration-split flow thin-cell fractionation (CFF-SPLITT). *Limnol. Oceanogr.* **45**: 1731–1742.
- HASEGAWA, T., I. KOIKE, AND H. MUKAI. 2001. Fate of food nitrogen in marine copepods. *Mar. Ecol. Prog. Ser.* **210**: 167–174.
- HEDGES, J. I. 1992. Global biogeochemical cycles: Progress and problems. *Mar. Chem.* **39**: 67–93.
- HEE, C. A., T. K. PEASE, M. J. ALPERIN, AND C. S. MARTENS. 2001. Dissolved organic carbon production and consumption in anoxic marine sediments: A pulsed-tracer experiment. *Limnol. Oceanogr.* **46**: 1908–1920.
- JACKSON, G. A., AND S. E. LOCHMANN. 1992. Effect of coagulation on nutrient and light limitation of an algal bloom. *Limnol. Oceanogr.* **37**: 77–89.
- KEMP, A. E. S., AND J. G. BALDAUF. 1993. Vast Neogene laminated diatom mat deposits from the eastern equatorial Pacific Ocean. *Nature* **362**: 141–144.
- KERNER, M., H. HOHENBERG, S. ERTL, M. RECKERMANN, AND A. SPITZY. 2003. Self-organization of dissolved organic matter to micelle-like microparticles in river water. *Nature* **422**: 150–154.
- KLEIN BRETELER, W. C. M., AND S. R. GONZALEZ. 1982. Influence of cultivation and food concentration on body length of calanoid copepods. *Mar. Biol.* **71**: 157–161.
- LANGE, C. B., S. K. BURKE, AND W. H. BERGER. 1990. Biological production off southern California is linked to climate change. *Climatic Change* **16**: 319–329.

- LEE, C., J. A. MCKENZIE, AND M. STURM. 1987. Carbon isotope fractionation and changes in the flux and composition of particulate matter resulting from biological activity during a sediment trap deployment in Lake Greifen, Switzerland. *Limnol. Oceanogr.* **32**: 83–96.
- LINDAHL, O. 1983. On the development of a *Gyrodinium aureolum* occurrence on the Swedish west coast in 1982. *Mar. Biol.* **77**: 143–150.
- . 1987. Plankton community dynamics in relations to water exchange in the Gullmar Fjord, Sweden. Ph.D. thesis, University of Stockholm.
- . 1995. Long-term studies of primary phytoplankton production in the Gullmar Fjord, Sweden, p. 105–112. In H. R. Skjoldal, C. Hopkins, K. E. Erikstad, and H. P. Leinaas [eds.], *Ecology of fjords and coastal waters*. Elsevier.
- LORRAIN, A., Y.-M. PAULET, L. CHAUVAUD, N. SAVOYE, A. DONVAL, AND C. SAOUT. 2002. Differential $\delta^{13}\text{C}$ and $\delta^{15}\text{N}$ signatures among scallop tissues: Implications for ecology and eco-physiology. *J. Exp. Mar. Biol. Ecol.* **275**: 47–61.
- MCCLELLAND, J. W., AND J. P. MONTOYA. 2002. Trophic relationships and the nitrogen isotopic composition of amino acids in plankton. *Ecology* **83**: 2173–2180.
- MCQUOID, M. R. 2002. Pelagic and benthic environmental controls on the spatial distribution of a viable diatom propagule bank on the Swedish west coast. *J. Phycol.* **38**: 881–893.
- MOORE, J. K., AND T. VILLAREAL. 1996. Size-ascent relationships in positively buoyant marine diatoms. *Limnol. Oceanogr.* **41**: 1514–1520.
- PARSONS, T. R., Y. MAITA, AND C. M. LALLI. 1984. A manual of chemical and biological methods for seawater analysis. Pergamon.
- PASSOW U., AND A. L. ALLDREDGE. 1994. Distribution, size and bacterial colonization of transparent exopolymer particles (TEP) in the ocean. *Mar. Ecol. Prog. Ser.* **113**: 185–198.
- POPP, B. N., E. A. LAWS, R. R. BIDIGARE, J. E. DORE, K. L. HANSON, AND S. G. WAKEHAM. 1998. Effect of phytoplankton cell geometry on carbon isotopic fractionation. *Geochim. Cosmochim. Acta.* **62**: 69–77.
- RIERA, P., L. J. STAL, AND J. NIEUWENHUIZE. 2002. $\delta^{13}\text{C}$ versus $\delta^{15}\text{N}$ of co-occurring mollusks within a community dominated by *Crassostrea gigas* and *Crepidula fornicata* (Oosterschelde, The Netherlands). *Mar. Ecol. Prog. Ser.* **240**: 291–295.
- ROLFF, C. 2000. Seasonal variation in $\delta^{13}\text{C}$ and $\delta^{15}\text{N}$ of size-fractionated plankton at a coastal station in the northern Baltic proper. *Mar. Ecol. Prog. Ser.* **203**: 47–65.
- SARMIENTO, J. L. 1991. Oceanic uptake of anthropogenic CO_2 : The major uncertainties. *Global Biogeochem. Cycles* **5**: 309–313.
- SMITH, V. H. 2002. Effects of resource supplies on the structure and function of microbial communities. *Antonie van Leeuwenhoek.* **81**: 99–106.
- TISELIUS, P., AND M. KUYLENSTIERNA. 1996. Growth and decline of a diatom spring bloom: Phytoplankton species composition, formation of marine snow and the role of heterotrophic dinoflagellates. *J. Plankton Res.* **18**: 133–155.
- UTERMÖHL, H. 1958. Zur vervollkommnung der quantitativen phytoplankton methodik. *Mitt. Int. Ver. Limnol.* **9**: 1–38.
- VAN DE BUND, W. J., E. ÓLAFSSON, H. MODIG, AND R. ELMGREN. 2001. Effects of the coexisting Baltic amphipods *Monoporeia affinis* and *Pontoporeia femorata* on the fate of a simulated spring diatom bloom. *Mar. Ecol. Prog. Ser.* **212**: 107–115.
- VAN DONGEN, B. E., S. SCHOUTEN, AND J. S. S. DAMSTÉ. 2002. Carbon isotope variability in monosaccharides and lipids of aquatic algae and terrestrial plants. *Mar. Ecol. Prog. Ser.* **232**: 83–92.
- VOLKMAN, J. K., AND E. TANOUE. 2002. Chemical and biological studies of particulate organic matter in the ocean. *J. Oceanogr.* **58**: 265–279.
- WAITE, A. M., P. K. BIENFANG, AND P. J. HARRISON. 1992a. Spring bloom sedimentation in a subarctic ecosystem I: Nutrients and sinking. *Mar. Biol.* **114**: 119–129.
- , P. A. THOMPSON, AND P. J. HARRISON. 1992b. Does energy control the sinking rates of marine diatoms? *Limnol. Oceanogr.* **37**: 468–477.
- , R. J. OLSON, H. DAM, AND U. PASSOW. 1995. Sugar-containing compounds on the cell surfaces of marine diatoms measured using Concanavalin A and flow cytometry. *J. Phycol.* **31**: 925–933.
- , A. FISHER, P. A. THOMPSON, AND P. J. HARRISON. 1997a. Sinking rate versus cell volume relationships illuminate sinking rate control mechanisms in marine diatoms. *Mar. Ecol. Prog. Ser.* **157**: 97–108.
- , S. M. GALLAGER AND H. DAM. 1997b. New measurements of phytoplankton aggregation in a flocculator using videography and image analysis. *Mar. Ecol. Prog. Ser.* **155**: 77–88.
- , K. SAFI, J. HALL, AND S. NODDER. 2000. Mass sedimentation of picoplankton embedded in organic aggregates. *Limnol. Oceanogr.* **45**: 87–97.

Received: 11 December 2003
 Accepted: 25 August 2004
 Amended: 30 November 2004